

## Fluorescence correlation spectroscopy in cells: Confinement and excluded volume effects

Iris von der Hocht, Jörg Enderlein\*

*Institute for Neurobiology and Biophysics 1, Forschungszentrum Jülich, D-52425 Jülich, Germany*

Received 17 December 2006, and in revised form 28 December 2006

Available online 12 January 2007

### Abstract

Fluorescence correlation spectroscopy (FCS) has become an important technique in biophysical research, which is also used for *in vivo* studies of molecular mobilities in cells. We theoretically study how confinement or exclusion of the diffusing fluorescent molecules by a spherical region influences the measured autocorrelation function in an FCS experiment. It is shown that close to the boundary of the spherical region the diffusion time can be significantly changed due to the geometric restriction of the detection volume. This is important when quantitatively evaluating and interpreting FCS measurements in cells.

© 2007 Elsevier Inc. All rights reserved.

### Introduction

Fluorescence correlation spectroscopy, invented in the 1970s by Magde et al. (1972), has evolved to a powerful and widely used tool for studying molecular mobility and interaction *in vitro* as well as *in vivo* (Rigler and Elson, 2001). In FCS, fluorescence fluctuations detected out of a very small detection volume (usually on the order of 1 fl or less) are recorded and then autocorrelated yielding the second order or autocorrelation function (ACF) of the fluctuating signal. If the average number of molecules within the detection volume is sufficiently small, the fluctuations are dominated by the random diffusion of the fluorescent molecules out of that volume, and the ACF shows a prominent decay which is characterized by the diffusion coefficient of the molecules. Thus, FCS can be used to determine the mobility of molecules within a sample, an issue of considerable interest in cell studies (Elson, 2001; Dittrich et al., 2001; Jankevics et al., 2005). However, the cellular environment is by far not homogeneous, which makes a quantitative evaluation of FCS data measured in live cells difficult and prone to misinterpretations (Verkman, 2002). There are numerous publications reporting e.g. the observation

of anomalous diffusion within cells (see e.g. Bacia and Schwille, 2003; Wachsmuth et al., 2000). However, as was pointed out by Egner et al. (1998), even small optical aberrations introduced by minute refractive index mismatches may cause a serious problem for correct FCS data evaluation when working in biological samples. Gennerich and Schild (2000) demonstrated that FCS in small cytosolic compartments can lead to gross errors in diffusion coefficients if confinement effects are not correctly taken into account. They considered FCS measurements on diffusing molecules confined in two dimensions. In the present paper, we will extend the work by Gennerich and Schild by modeling FCS measurements on fluorescing molecules that diffuse within or around a spherical compartment. This can be, for example, proteins diffusing within or around vacuoles or other spherical organelles which are present in high density and large size variations in any living cell. We present numerical results which will help to estimate the potential errors made when using FCS for quantifying molecular mobilities.

### Materials and methods

#### *Modeling FCS in a spherical confinement*

In FCS, the detected fluorescence intensity is correlated with a time-shifted replica of itself at different values of time shift  $\tau$ . The result is the so-called

\* Corresponding author.

E-mail address: [j.enderlein@fz-juelich.de](mailto:j.enderlein@fz-juelich.de) (J. Enderlein).

URL: <http://www.joerg-enderlein.de> (J. Enderlein).

autocorrelation function (second-order correlation function) which is calculated as

$$g(\tau) = \langle I(t)I(t+\tau) \rangle_t \quad (1)$$

where  $I(t)$  is the detected fluorescence intensity at time  $t$ , and the triangular brackets denote averaging over all time values  $t$ . The calculation of the ACF is equivalent to determining the probability to detect a photon at time  $t+\tau$  if there was a photon detected at time  $t$ . In the present paper, we focus on FCS within and around spherical enclosures and would like to study how the diffusion governed part of the ACF is changed by the presence of the spherical enclosure. Thus, we completely neglect any photophysical or conformational processes that might also affect the ACF. A purely diffusion-generated ACF can be calculated as follows (see Enderlein et al., 2005 for the details)

$$g(\tau) = c \int dr_1 \int dr_0 U(r_1) G(r_1, r_0, \tau) U(r_0) + \left[ c \int dr U(r) \right]^2, \quad (2)$$

where  $c$  denotes the concentration of fluorescent molecules,  $U(r)$  is the so-called molecule detection function (MDF) which describes with which probability a fluorescence photon is excited and detected for a molecule at position  $r$  within the sample, and  $G(r_1, r_0, \tau)$  is Green's function of the diffusion equation for the given boundary conditions.  $G(r_1, r_0, \tau)$  is the probability density that a molecule diffuses from position  $r_0$  to position  $r_1$  within time  $\tau$ . Thus, for calculating the ACF one needs to know the MDF,  $U(r)$ , and Green's function,  $G(r_1, r_0, \tau)$ . When neglecting minor effects connected with fluorescence anisotropy (i.e. slow rotational diffusion leading to a correlation between the absorption and emission dipole orientation during excitation and fluorescence emission, respectively) (Enderlein et al., 2004), the MDF is given by the product of excitation intensity distribution and fluorescence collection efficiency function. We calculated both functions and thus the MDF using exact wave-optical modeling as explained in detail in Enderlein et al. (2005). Green's function,  $G(r_1, r_0, \tau)$ , is found as a solution of the three-dimensional diffusion equation,

$$\frac{\partial G}{\partial t} = D\Delta G \quad (3)$$

with appropriate boundary and initial conditions. In the above equation,  $D$  denotes the diffusion coefficient, and  $\Delta$  the three-dimensional Laplace operator. When modeling diffusion within or around a confining sphere, one has vanishing flux across the sphere surface so that the boundary condition reads

$$\frac{\partial G}{\partial r} \Big|_{r=a} = 0 \quad (4)$$

where  $r$  is the radial coordinate in a spherical coordinate system with its origin at the center of the sphere, and  $a$  is the sphere's radius. The initial condition demands that the diffusion starts exactly at position  $r_0$  at time  $t=0$ , i.e.

$$G(r_1, r_0, t=0) = \delta(r_1 - r_0). \quad (5)$$

where  $\delta(r)$  is the three-dimensional Dirac function. The exact solution for  $G(r_1, r_0, \tau)$  is given by the following infinite series expansion (Morse and Feshbach, 1953)

$$G(r_1, r_0, \tau) = \sum_{n=0}^{\infty} \sum_{m=-n}^n \sum_{\alpha=0}^{\infty} c_{n,\alpha} \psi_{n,m,\alpha}(r_1, \theta_1, \phi_1) \bar{\psi}_{n,m,\alpha}(r_0, \theta_0, \phi_0) \times \exp[-Dk_{n,\alpha}^2 \tau] \quad (6)$$

where  $r \equiv \{r, \theta, \phi\}$  are spherical coordinates, a bar denotes complex conjugation, the eigenfunctions  $\psi_{n,m,\alpha}(r, \theta, \phi)$  are defined by

$$\psi_{n,m,\alpha}(r, \theta, \phi) = Y_{nm}(\theta, \phi) j_n(k_{n,\alpha} r) \quad (7)$$

with  $Y_{nm}(\theta, \phi)$  denoting spherical harmonic functions (Abramowitz and Stegun, 1984),

$$Y_{nm}(\theta, \phi) = \sqrt{\frac{2l+1(l-|m|)!}{4\pi(l+|m|)!}} P_l^{|m|}(\cos\theta) \exp(im\phi) \quad (8)$$

with  $P_l^m$  being associated Legendre functions (Abramowitz and Stegun, 1984);  $j_n$  are spherical Bessel functions of the first kind (Abramowitz and Stegun, 1984); the  $k_{n,\alpha}$  are defined by the transcendental equation

$$\frac{\partial j_n(k_{n,\alpha} r)}{\partial r} \Big|_{r=a} = 0, \quad (9)$$

with  $\alpha$  enumerating the infinite number of solutions of this equations in ascending order; and the normalizing factors  $c_{n,m,\alpha}$  are given by

$$c_{n,\alpha} = \frac{2}{a^3} \left[ \left( 1 - \frac{n(n+1)}{k_{n,\alpha}^2 a^2} \right) j_n^2(k_{n,\alpha} a) \right]^{-1} \quad (10)$$

if  $k_{n,\alpha} > 0$  and  $c_{0,0} = 3/a^3$  (having  $k_{0,0} = 0$ ). Using this solution, the time-dependent part of the ACF, i.e. the first term on the r.h.s. of Eq. (2), can be calculated as

$$g(\tau) - g_{\infty} = \sum_{n,m,\alpha} c_{n,m,\alpha} \exp(-Dk_{n,\alpha}^2 \tau) \Big|_{V_S} \int dr U(r) \psi_{n,m,\alpha}(r) \Big|^2, \quad (11)$$

where  $g_{\infty}$  denotes the ACF value at  $\tau \rightarrow \infty$ , and the integration is performed over the sphere's volume  $V_S$ . Thus, the calculation of the ACF reduces to a summation over squares of integrals, which have to be evaluated numerically.

For making a quantitative comparison of the apparently observed molecular mobility for different focus positions with respect to the confining sphere, we determined the *diffusion time*  $\tau_{1/2}$  defined by

$$g(\tau_{1/2}) - g_{\infty} = \frac{1}{2} [g(0) - g_{\infty}], \quad (12)$$

i.e.  $\tau_{1/2}$  is the time where the time-dependent part of the ACF has fallen off to half of its initial value.

### Modeling FCS around a spherical exclusion

Calculating the ACF for diffusion in an infinite volume where a spherical region is excluded is similar to the previous section. However, now the eigenfunctions  $\psi_{n,m,\alpha}$  have the modified form

$$\psi_{n,m,k}(r, \theta, \phi) = Y_{nm}(\theta, \phi) \frac{y_n'(ka) j_n(kr) - j_n'(ka) y_n(kr)}{\sqrt{y_n'^2(ka) + j_n'^2(ka)}} \quad (13)$$

where the  $y_n$  are spherical Bessel functions of the second kind (Abramowitz and Stegun, 1984), a prime denotes differentiation, and Green's function is now represented by a double sum and integral instead of a triple sum,

$$G(r_1, r_0, \tau) = \frac{2}{\pi} \sum_{n=0}^{\infty} \sum_{m=-n}^n \int_0^{\infty} dk k^2 \psi_{n,m,k}(r_1, \theta_1, \phi_1) \bar{\psi}_{n,m,k}(r_0, \theta_0, \phi_0) \exp[-Dk^2 \tau]. \quad (14)$$

The final result for the ACF looks similar to the previous section,

$$g(\tau) - g_{\infty} = \frac{2}{\pi} \sum_{n,m} \int_0^{\infty} dk k^2 \exp(-Dk^2 \tau) \Big|_{V_o} \int dr U(r) \psi_{n,m,k}(r) \Big|^2, \quad (15)$$

where the integration extends over the whole space  $V_o$  outside the sphere. This expression has again to be evaluated numerically.

## Results and discussion

The general situation studied is shown in Fig. 1: a focused laser beam together with confocal detection of the excited fluorescence generates a small and well defined detection volume where fluorescence can be efficiently detected. By monitoring fluorescence fluctuations caused by molecules diffusing in and out of that volume, and by determining how fast the autocorrelation of these fluctuations decays, one

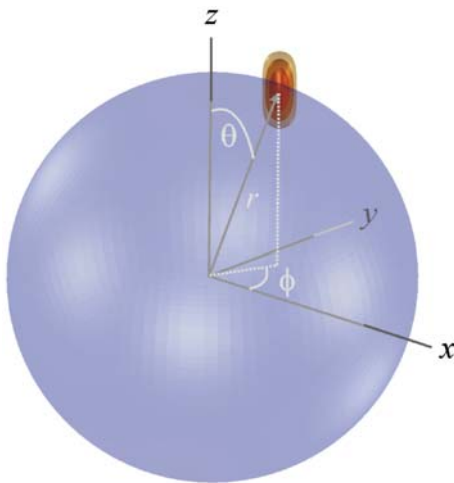


Fig. 1. General geometry of the considered experiment: a confocal detection volume is positioned close or onto a spherical region that confines or excludes diffusing fluorescent molecules. The resulting autocorrelation function and diffusion time are calculated as a function of the position  $(r, \theta, \phi)$  of the detection volume with respect to the sphere's center.

quantifies the mobility of the diffusing molecules. However, when the detection volume is situated close to a boundary that restricts the diffusive motion of the molecules, i.e. if some part of the detection volume is cut off by the boundary, the temporal decay of the fluorescence autocorrelation is changed, and thus the *apparent* mobility of the molecules. For a spherical boundary, two cases can be considered: the diffusing molecules are enclosed by the boundary (confinement), or the molecules are excluded from the spherical region (exclusion). We will quantify, for both cases, the influence of the boundary on an FCS measurement by calculating the diffusion time  $\tau_{1/2}$ , defined by Eq. (12), as a function of the relative position of the detection volume with respect to the spherical boundary.

First, we have to specify the MDF which will be used for the calculations. We computed the MDF using an exact wave-optics approach as described in Enderlein et al. (2005). The computations were done for an aberration-free water immersion objective with 1.2 numerical aperture. Fluorescence imaging onto the confocal aperture was assumed to be performed with  $60\times$  magnification, aperture diameter was set to  $20\ \mu\text{m}$ . Laser beam diameter was set equal to the diameter of the objective's back aperture, resulting in laser focusing close to the diffraction limit. The calculations were performed for 635 nm excitation and 670 nm emission wavelengths. The resulting shape of the MDF is visualized in Fig. 2.

Knowing the MDF  $U(r)$  and using Eqs. (11) and (12), we calculated the diffusion time  $\tau_{1/2}$  as a function of relative position of the detection volume with respect to a confining sphere of radius  $a$ . The different values of  $a$  were studied, namely  $a=0.5, 1$  and  $2\ \mu\text{m}$ . The results for the three radius values are shown in Figs. 3A–C. In each panel, the left side shows the fluorescence intensity as a function of focus position relative to the boundary, and the right side shows the diffusion time  $\tau_{1/2}$  as a function of this position. A remarkable result is

that, when the detection volume crosses the enclosing boundary, the diffusion time  $\tau_{1/2}$  *increases* although more and more of the detection volume is cut off by the boundary. This can be understood when realizing that  $\tau_{1/2}$  is mainly determined by the largest gradient of the MDF, i.e. how fast the MDF changes from point to point. If the center of the MDF is cut off by the boundary, the remaining part has much shallower gradients than the full distribution leading to an apparently slower decay of the autocorrelation function. As can be seen from Figs. 3B–C, the *apparent* slowdown of molecular mobility can be more than a factor of 2.5, although it occurs when the fluorescence intensity has dropped of to only a few percent of its value in free solution. Thus, the presence of the spherical enclosure induces a shell of apparently less mobile molecules near its surface. This is, of course, a purely geometrical effect and has nothing to do with the actual diffusion speed of the molecules, which is assumed to be everywhere the same.

An interesting question is whether one can recognize the position of the focus with respect to the boundary by inspecting the shape of the ACF. Fig. 3D shows a series of ACFs for different focus positions when moving the focus across the interface along the optical axis. What can be seen is that the *shape* of the different ACFs is rather similar although the diffusion time shifts significantly. Thus, the shape of the ACF cannot give decisive information about the exact focus position with respect to the boundary, which will make the recognition of boundary effects in praxis rather difficult.

Next, we calculated, using Eqs. (12) and (15),  $\tau_{1/2}$  as a function of relative position of the focus position with respect to an *excluding* sphere of radius  $a$ . Again, we considered three radius values, this time  $a=0.2, 0.5,$  and  $1\ \mu\text{m}$ . The computational result is shown in Figs. 4A–C. Remarkably, for small radius values the impact of the excluded volume on the apparent mobility is less than one could expect: although the

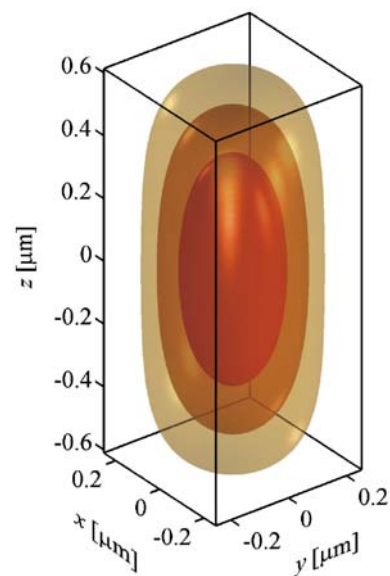


Fig. 2. Shape of the molecule detection function used for the calculations. Shown are three iso-surfaces corresponding to fluorescence excitation times detection probabilities of  $1/e, 1/e^2,$  and  $1/e^3,$  respectively.

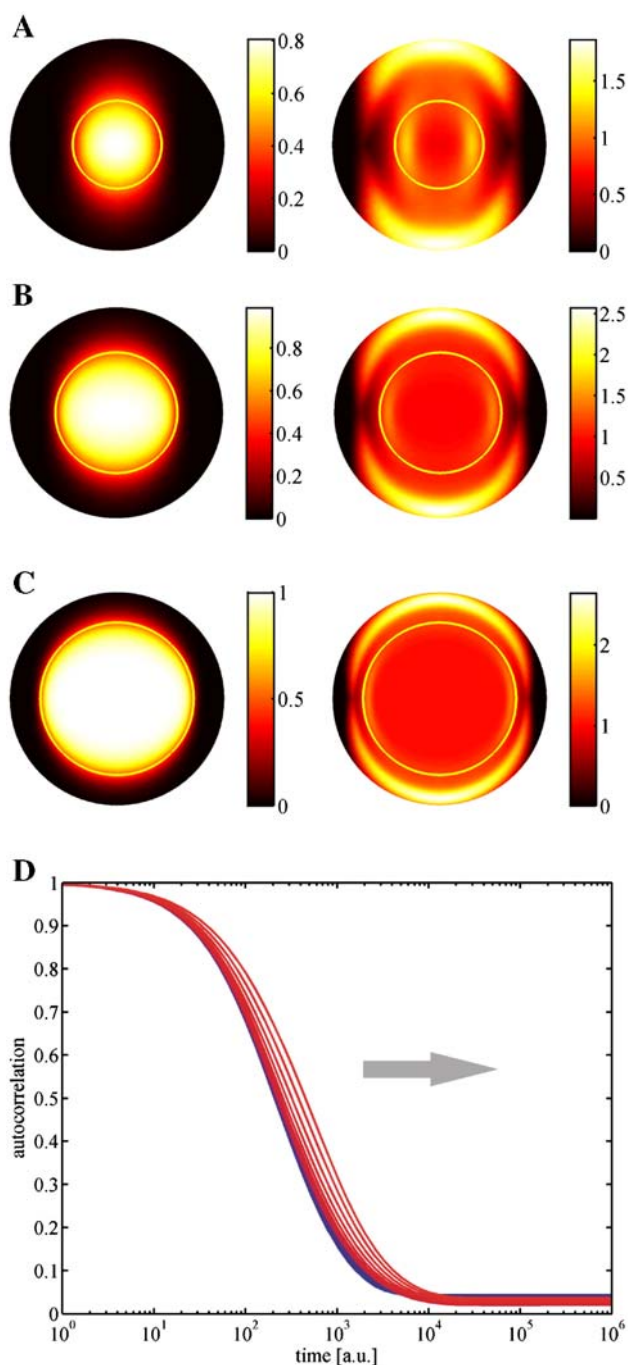


Fig. 3. (A) Dependence of relative intensity (left) and diffusion time (right) on position of the detection volume (focus position) with respect to a confining sphere of radius  $0.5 \mu\text{m}$ . The color bars indicate the values of intensity (left) and diffusion time (right) in units of intensity and diffusion time for an unrestricted volume, respectively. The circle indicates the boundary of the confining sphere. (B) Same as in panel A but for a confining sphere of radius  $1 \mu\text{m}$ . (C) Same as in a but for a confining sphere of radius  $2 \mu\text{m}$ . (D) Shape of the normalized ACFs when moving the focus along the optical axis across the boundary of a confining sphere of  $1 \mu\text{m}$ . Shown are curves for focus positions from  $z=0 \mu\text{m}$  up to  $z=1.5 \mu\text{m}$  in steps of  $0.05 \mu\text{m}$ . The arrow indicates the shift of the ACFs with increasing  $z$ -position.

spatial extension of the detection volume is only ca.  $1 \mu\text{m}$  along the optical axis and ca.  $0.4 \mu\text{m}$  perpendicular to the optical axis, the presence of an excluding sphere of  $0.4 \mu\text{m}$

diameter does not have a significant effect on the apparent diffusion time. Only for sphere diameters around  $1 \mu\text{m}$  and larger, the diffusion time is altered significantly, in a similar way as for the confining sphere but with opposite location. As in the case of the confining volume, the shape of the ACFs is similar for most focus positions (not shown), making it again rather difficult to recognize the presence of a boundary effect in an FCS measurement based on the shape of the measured ACF.

### Conclusion

We have presented exact theoretical modeling of the geometric effect of an enclosing or excluding sphere on the measured diffusion time in an FCS experiment. As was seen, the presence of the geometric restriction leads most prominently to an *apparent* slowdown of molecular mobility close to the boundary. Taking into account that we considered a very simple geometric configuration, whereas in real cells lipid boundaries of organelles and vesicles abound, it can be expected that such cut-off effects of the detection volume have significant impact on FCS measurements in cells. Moreover, we have considered only the effect of geometric restriction of diffusion, whereas in a cellular environment, organelles or vacuoles may have sig-

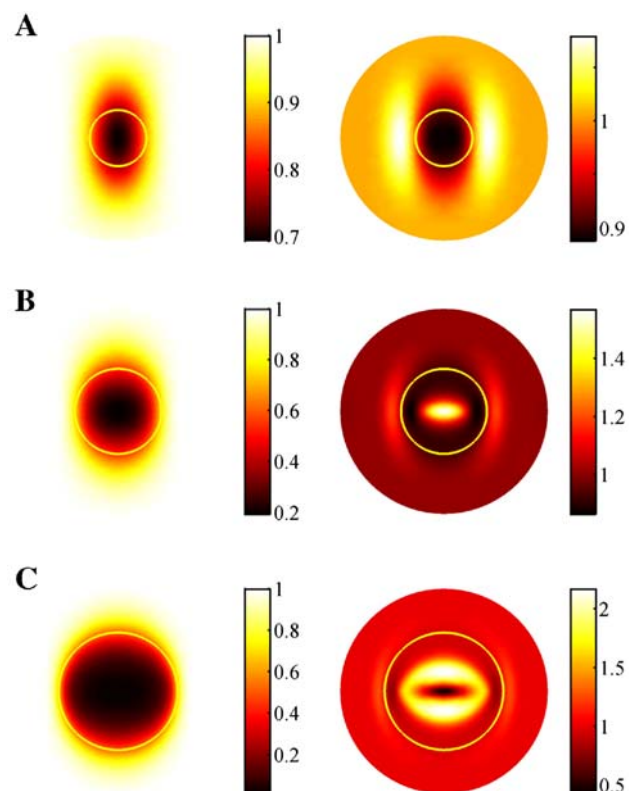


Fig. 4. (A) Dependence of relative intensity (left) and diffusion time (right) on position of the detection volume with respect to an excluding sphere of radius  $0.2 \mu\text{m}$ . The color bars indicate the values of intensity (left) and diffusion time (right) in units of intensity and diffusion time for an unrestricted volume, respectively. The circle indicates the boundary of the confining sphere. (B) Same as in a but for an excluding sphere of radius  $0.5 \mu\text{m}$ . (C) Same as in panel A but for an excluding sphere of radius  $1 \mu\text{m}$ .

nificantly different refractive index values than that of the surrounding cytoplasm, introducing additional optical aberrations which will distort the MDF and thus the resulting ACF. Thus, when interpreting FCS measurements in cells one should be careful to take into account geometric restriction effects (and also optical aberrations due to refractive index variations) before trying to evoke more arcane explanations such as anomalous diffusion.

### Acknowledgments

We thank Thomas Dertinger and Ingo Gregor for many helpful discussions. Financial support by the Deutsche Forschungsgemeinschaft is gratefully acknowledged.

### References

- Abramowitz, M., Stegun, I.A., 1984. *Handbook of Mathematical Functions*. Harry Deutsch, Thun.
- Bacia, K., Schwille, P., 2003. A dynamic view of cellular processes by in vivo fluorescence auto- and cross-correlation spectroscopy. *Methods* 29, 74–85.
- Dittrich, P., Malvezzi-Campeggi, F., Jahnz, M., Schwille, P., 2001. Accessing molecular dynamics in cells by fluorescence correlation spectroscopy. *Biol. Chem.* 382, 491–494.
- Egner, A., Schrader, M., Hell, S.W., 1998. Refractive index mismatch induced intensity and phase variations in fluorescence confocal, multiphoton and 4Pi-microscopy. *Opt. Commun.* 153, 211–217.
- Elson, E.L., 2001. Fluorescence correlation spectroscopy measures molecular transport in cells. *Traffic* 2, 789–796.
- Enderlein, J., Gregor, I., Patra, D., Fitter, J., 2004. Art and artefacts of fluorescence correlation spectroscopy. *Curr. Pharm. Biotechnol.* 5, 155–161.
- Enderlein, J., Gregor, I., Patra, D., Dertinger, T., Kaupp, U.B., 2005. Performance of fluorescence correlation spectroscopy for measuring diffusion and concentration. *ChemPhysChem* 6, 2324–2336.
- Gennerich, A., Schild, D., 2000. Fluorescence correlation spectroscopy in small cytosolic compartments depends critically on the diffusion model used. *Biophys. J.* 79, 3294–3306.
- Jankevics, H., Prummer, M., Izewska, P., Pick, H., Leufgen, K., Vogel, H., 2005. Diffusion-time distribution analysis reveals characteristic ligand-dependent interaction patterns of nuclear receptors in living cells. *Biochemistry* 44, 11676–11683.
- Magde, D., Elson, E., Webb, W.W., 1972. Thermodynamic fluctuations in a reacting system—measurement by fluorescence correlation spectroscopy. *Phys. Rev. Lett.* 29, 705–708.
- Morse, P.M., Feshbach, H., 1953. *Methods of Theoretical Physics*. McGraw-Hill, New York.
- Rigler, R., Elson, E.S., 2001. *Fluorescence Correlation Spectroscopy: Theory and Applications*. Springer, Berlin, Germany.
- Verkman, A.S., 2002. Solute and macromolecule diffusion in cellular aqueous compartments. *Trends Biochem. Sci.* 27, 27–33.
- Wachsmuth, M., Waldeck, W., Langowski, J., 2000. Anomalous diffusion of fluorescent probes inside living cell nuclei investigated by spatially resolved fluorescence correlation spectroscopy. *J. Mol. Biol.* 298, 677–689.